

Mechanism of Cytotoxicity of Copper(I) Complexes of 1,2-Bis(diphenylphosphino)ethane

Nusrat J. Sanghamitra,[†] Pornima Phatak,[‡] Sanjeev Das,[‡] Ashoka G. Samuelson,^{*,†} and Kumaravel Somasundaram^{*,‡}

Department of Inorganic and Physical Chemistry and Department of Microbiology and Cell Biology, Indian Institute of Science, Bangalore 560 012, India

Received July 17, 2004

The cytotoxic properties of arylphosphines are regulated by metals. We have synthesized a series of copper(I) complexes of 1,2-bis(diphenylphosphino)ethane (DPPE) and tested their in vitro cytotoxicity in a human lung carcinoma cell line H460. One of the complexes $[\text{Cu}_2(\text{DPPE})_3(\text{CH}_3\text{CN})_2](\text{ClO}_4)_2$ (C1), showed maximum cytotoxicity comparable to that of adriamycin. Treatment of cells with C1 caused DNA damage in vitro and activated the p53 pathway. Flow cytometry revealed that growth inhibition by C1 was due to a combination of cell cycle arrest and apoptosis. Simultaneous addition of C1 and adriamycin increased the cytotoxicity of either compound, suggesting the potential use of adriamycin in combination with C1. DNA binding and simulation studies suggest that adriamycin binds to DNA synergistically in the presence of C1. Thus, we have identified C1, a copper(I) complex of DPPE, as a potential chemotherapeutic drug for further testing, which could be used either alone or in combination with other chemotherapeutic drugs.

Introduction

Cisplatin is one of the most widely used metallodrugs for solid tumors. Despite its success, clinical use of cisplatin is limited due to acquired and intrinsic resistance of cancer cells to the drug and its high toxicity to some normal cells.¹ Hence, there exists an immense interest to improve the design of metallodrugs having reduced toxicity and a high spectrum of activity, especially drugs that would show activity against cell lines resistant to cisplatin. A group of complexes that are particularly relevant in this regard are the phosphine complexes of group 11 metal ions. Their biological properties were relatively unexplored until the late 1970s when a thioglucose derivative of triethyl phosphine gold(I) (auranofin) was found to be antiarthritic and subsequently shown to have in vivo antitumor activity, although only against P388 leukemia.² In an attempt to identify gold-containing complexes with a wider spectrum of activity, extensive work done by Sadler's group demonstrated the cytotoxicity of $\text{Au}(\text{DPPE})_2\text{Cl}$ in several cell lines such as B16 melanoma, P388 leukemia, and M5076 reticulum cell carcinoma (DPPE = 1,2-bis(diphenylphosphino)ethane).³ It was found that DPPE–gold complexes were 10-fold more cytotoxic than DPPE alone, suggesting that metal ions potentiate the cytotoxic property of DPPE.⁴ In addition, the cytotoxic properties of DPPE were found to be increased by Au^{III} and Cu^{II} but not by Mg^{II} , Zn^{II} , Mn^{II} , Fe^{II} , Co^{II} , and Cd^{II} .⁴ Nephrotoxicity associated with the phenyl groups on DPPE could also be a reason these complexes have not been investigated more extensively.⁵

In our previous study, we demonstrated the in vitro antitumor activity against PA1, CHO, and human ovarian carcinoma cell lines by analogous copper(I) complexes of phosphines and heterocyclic thiones.⁶ One of the complexes $\text{Cu}_2(\text{DPPE})_3(\text{CH}_3\text{CN})_2(\text{ClO}_4)_2$ (C1) was found to be more active than adriamycin.⁶ The promising activity and reactivity of C1 prompted us to investigate a series of copper(I) DPPE complexes. There exists a broad consensus about the importance of platinum–DNA interaction in the working mechanism of cisplatin.⁷ However, significant differences in the reactivity of metallodrugs and the redox properties make it difficult to predict pathways of action without specific investigations. Hence, mechanistic studies based on cell cycle analysis supported by in vitro reactivity studies would go a long way in the design of new anticancer copper(I) complexes. Recent studies by Pillarsetty et al. on the cell arrestation properties of a gold complex illustrate the value of such studies.⁸ Mechanistic studies are also likely to help one design a metal complex with less toxicity.

In this report, we describe the synthesis of several Cu^{I} DPPE complexes, with and without N-heterocycles such as carbazole and benzotriazole, and the study on the mechanism of cytotoxicity against H460, a human lung carcinoma cell line. The most active complex was found to be $[\text{Cu}_2(\text{DPPE})_3(\text{CH}_3\text{CN})_2](\text{ClO}_4)_2$ (C1). We found C1 damaged DNA in vitro and activated the p53 pathway. We also showed that C1 inhibits the growth of cancer cells by inducing cell cycle arrest and apoptosis. In addition, C1 and adriamycin worked synergistically by potentiating the cytotoxicity of one by the other. Finally, we found evidence through binding and simulation studies for increased binding of adriamycin

* Authors to whom correspondence should be addressed. Phone: 91-80-22932663 (A.S.). Fax: 91-80-23601552 (A.S.). E-mail: ashoka@ipc.iisc.ernet.in. Phone: 91-80-22932973 (K.S.). Fax: 91-80-23602697 (K.S.) E-mail: skumar@mcbl.iisc.ernet.in.

[†] Department of Inorganic and Physical Chemistry.

[‡] Department of Microbiology and Cell Biology.

Table 1. IC₅₀ Values of Different Copper(I) Complexes of DPPE

no.	compound	IC ₅₀ ^a
1	adriamycin	0.05 (0.002)
2	C1	0.07 (0.02)
3	C2	0.55 (0.12)
4	C3	0.55 (0.1)
5	C4	0.54 (0.07)
6	DPPE	0.25 (0.04)

^a Refers to amount of drug in $\mu\text{g}/\text{mL}$ to inhibit the growth of H460 cells by 50% in 48 h. Each value is the average of three sets of experiments.

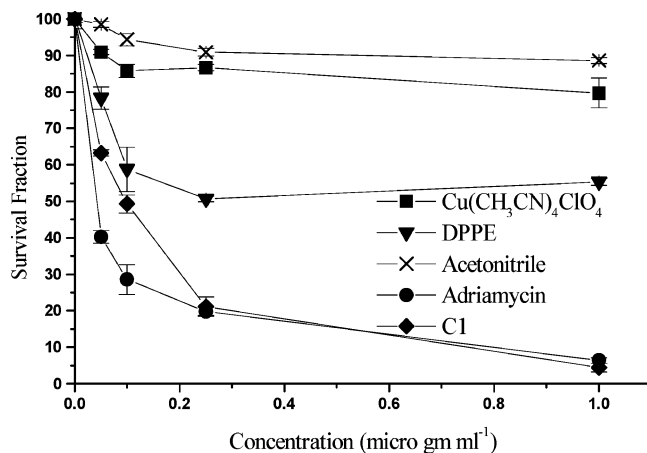


Figure 1. Cytotoxicity of C1. H460 cells were treated with increasing concentrations (0.05, 0.1, 0.25, and 1 $\mu\text{g}/\text{mL}$) of acetonitrile, CAP, DPPE, adriamycin, and C1. After 48 h of addition of these compounds, the proportion of live cells was quantified by the MTT assay as described in the Experimental Section. The absorbance of control cells was considered as 100%.

to DNA modified by C1, thus providing a plausible mechanism for synergistic action between adriamycin and C1.

Results

Cytotoxicity of Copper(I) Complexes of DPPE.

H460 cells were cultured in the presence of varying concentrations of different copper(I) complexes of DPPE for 48 h, and the cytotoxicity was analyzed by MTT assay (MTT = 3-(4,5-dimethylthiazol-2-yl)-2,5-diphenyltetrazolium bromide). Adriamycin was used as a positive control. The IC₅₀ values for all of the compounds were determined and are given in Table 1. Of all of the copper(I) complexes tested, C1 had an IC₅₀ value of 0.07 $\mu\text{g}/\text{mL}$, which was similar to that of adriamycin (0.05 $\mu\text{g}/\text{mL}$) (Figure 1, Table 1). All of the other compounds tested had considerably higher IC₅₀ values. We also tested appropriate ligands as well as DPPE used in the synthesis of C1 for their cytotoxicity. Acetonitrile and $\text{Cu}(\text{CH}_3\text{CN})_4\text{ClO}_4$ did not inhibit the growth of cells (Figure 1). However, DPPE had an IC₅₀ value of 0.25 $\mu\text{g}/\text{mL}$ (Figure 1, Table 1). These results suggest that the cytotoxicity of DPPE is further enhanced by copper in C1 by about 3.6-fold. Because the activity of C1 was found to be in the range of adriamycin, we decided to test its mechanism of action.

C1 Damages DNA in Vitro and Activates the p53 Pathway. To find out whether C1 causes damage to DNA in vitro, we carried out a single cell gel electrophoresis (COMET assay) of cells treated with C1.

Adriamycin was used as a positive control as it has been shown to intercalate DNA and cause damage to DNA possibly by inhibiting the topoisomerase II enzyme.^{9–11} Adriamycin addition resulted in the formation of comets (Figure 2A compare panel b with a) in about 93.6% of treated cells (Table 2) in comparison to untreated cells (8.65%). Similarly, comets were seen in 90.6% of C1 treated H460 cells (Figure 2A compare panel c with a, Table 2).

DNA damage has been shown to inhibit the growth of cells by inducing the tumor suppressor p53. Because our results suggest that C1 causes DNA damage, we investigated the ability of C1 to activate the p53 pathway. First, we checked the effect of C1 on the levels of p53. H460 cells were treated with adriamycin and C1, and the cells were stained for p53 by immunohistochemistry. Adriamycin-treated cells induced high levels of p53 in comparison to untreated control cells (Figure 2B compare panel b with a). Similarly, C1-treated cells show high levels of p53 (Figure 2B compare panel c with a). To see whether C1-induced p53 is functional, we monitored the levels of p21^{WAF1/CIP1}, a known transcriptional target of p53. Adriamycin as well as C1 treatment resulted in an increase in levels of p21^{WAF1/CIP1} in comparison to that in untreated cells (Figure 2B compare panels e and f with d). These results suggest that C1 causes DNA damage in vitro and activates the p53 pathway.

C1 Induces Cell Cycle Arrest and Apoptosis.

Upon induction, p53 is known to arrest the growth of cells and induce apoptosis.¹² Because our results show C1 is growth inhibitory and it activates the p53 pathway, we decided to check the ability of C1 to induce growth arrest and apoptosis. First, we carried out [³H]-thymidine incorporation to monitor cellular DNA synthesis in C1-treated cells. Treatment of H460 cells with C1 resulted in dose-dependent inhibition of DNA synthesis (Figure 2D compare bars 2–5 with 1) as seen by decreasing [³H]thymidine incorporation as the concentration of drug is increased. C1 treatment also resulted in apoptosis induction as seen by bright blue fluorescence upon DAPI staining, which is indicative of nuclear fragmentation (Figure 2C compare panel c with a). Adriamycin, which was used as positive control, also induced apoptosis (Figure 2C compare panel b with a). To confirm these observations, we studied the cell cycle profile of C1-treated cells by fluorescence-activated cell sorting (FACS). Treatment of cells with increasing concentrations of C1 for 48 h resulted in accumulation of cells with 2N and 4N amounts of DNA, suggesting the arrest of cells in the G1 and G2/M phases of the cell cycle (Figure 3, parts A and C). Arrest of cells in the G1 and G2/M phases of the cell cycle also resulted in concomitant decrease in S-phase populations. In addition to these changes, there was also the appearance of cells possessing less than 2N amount of DNA, which represent cells undergoing apoptosis (Figure 3, parts A and C). Next, we treated H460 cells with 1.0 $\mu\text{g}/\text{mL}$ of C1 for different time points and analyzed the cell cycle profile by FACS. Accumulation of cells particularly at the G2/M phase of the cell cycle was evident as early as after 24 h of treatment, becoming very obvious by 48 h (Figure 3, parts B and D). However, the apoptotic cells appeared only after 48 h (10.54%)

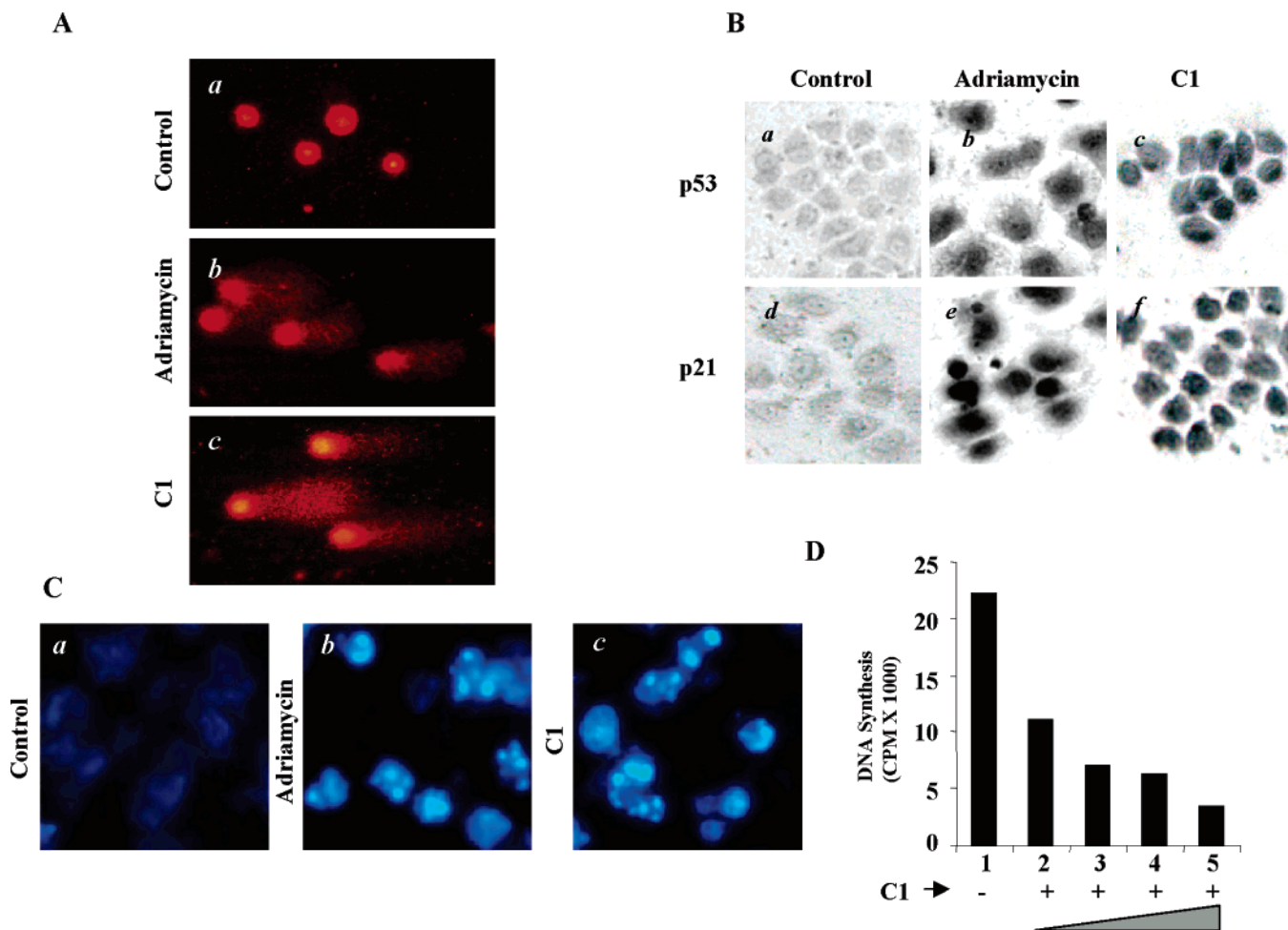


Figure 2. (A) C1 causes DNA damage in vitro. H460 cells were treated with (b) adriamycin and (c) C1 for 24 h, and the cells were subjected to the COMET assay. Comets are visualized under a fluorescent microscope. (B) C1 induces p53 and p21 levels. H460 cells were treated with adriamycin (b and e) or C1 (c and f) for 24 h. The cells were fixed and analyzed by immunohistochemical staining for p53 (a, b, and c) or p21 (d, e, and f). (C) H460 cells were treated with (b) adriamycin or (c) C1. After 48 h of addition of these compounds, 1 μ L of 1 mg/mL DAPI was added to each well, and they were observed under UV microscopy immediately. Note that the spots with bright blue fluorescence in panels b and c indicate the presence of nuclear fragmentation. (D) H460 cells were treated with increasing amounts of C1 (0.05, 0.1, 0.25, and 1 μ g/mL). The cells were allowed to incorporate [3 H]thymidine for the last 4 h of the time points at which they were collected. After 24 h of addition of C1, [3 H]thymidine incorporated into cellular DNA was measured as described in the Experimental Section.

Table 2. Results of Single Cell Gel Electrophoresis

no.	compound	% of cells with COMET ^a
1		9.28 (0.69)
2	adriamycin	93.55 (1.21)
3	C1	90.60 (3.37)

^a Refers to the average % of cells with COMET, calculated from three sets of experiments.

and have further increased to high levels (22.34%) by 72 h (Figure 3, parts B and D). These experiments suggest that C1 inhibits the growth of H460 cells by inducing cell cycle arrest as well as apoptosis.

Synergism between C1 and Adriamycin. Combination therapy has been found to be extremely effective. Testicular cancer has become a model for curable neoplasm by using a combination of cisplatin, vinblastin, and bleomycin.¹³ Because adriamycin and C1 are potent inhibitors of cancer cell growth individually, we decided to check whether a combination of C1 and adriamycin could function in a synergistic fashion to inhibit the growth of H460 cells. Cells were treated with increasing concentrations of C1 in the presence of a constant amount of adriamycin and vice versa, and the cytotoxicity

of each of the compounds was analyzed by the MTT assay (Figure 4, parts A and B). In the presence of a constant amount of adriamycin, the cytotoxicity of C1 was enhanced significantly (Figure 4A, 0.07–0.02 mg/mL). Similarly, the presence of C1 also enhanced the cytotoxicity of adriamycin, although less significantly (Figure 4B). We conclude from these experiments that adriamycin and C1 work synergistically. To support the synergistic effect between adriamycin and C1, an isobologram analysis was carried out to see the effects of one drug on the action of the other. Zero interaction response curves were calculated using the median effect relation.^{14,15} The predicted zero interaction curves for C1 in the presence of a constant amount of adriamycin and vice versa are shown (Figure 4, parts C and D, respectively). The experimental curve for the combination of C1 and adriamycin, when the later is added in constant amounts with variable concentrations of C1, is much below the zero interaction curve (Figure 4C). Similarly, when C1 is added in constant amounts with variable concentrations of adriamycin, the experimental curve also deviates from the zero interaction curve but

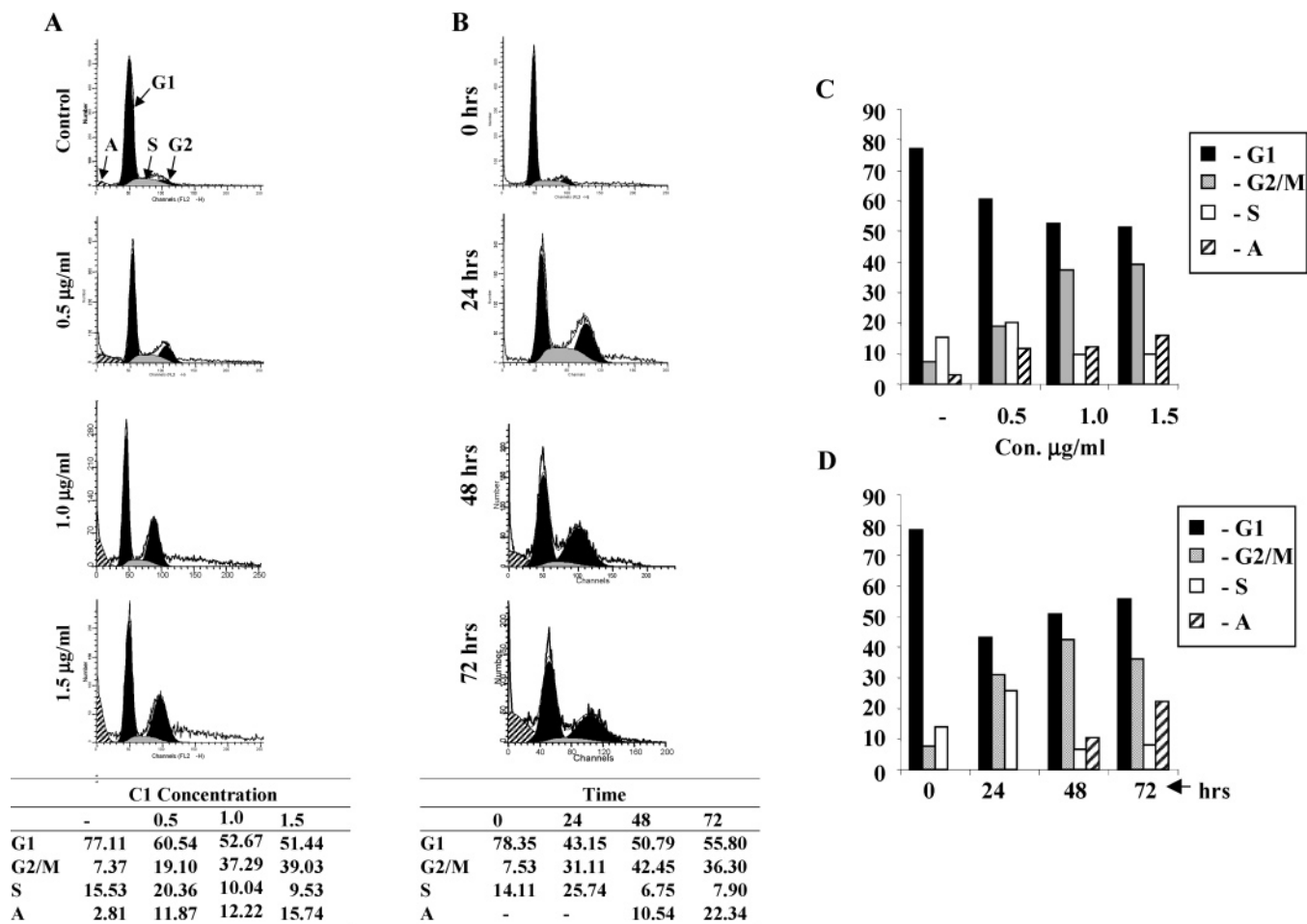


Figure 3. Induction of cell cycle arrest and apoptosis in C1-treated cells. (A) H460 cells were treated with different concentrations of C1, and the cells were harvested after 48 h and subjected to flow cytometry analysis as mentioned in the Experimental Section. (B) H460 cells were treated with 1 $\mu\text{g}/\text{mL}$ of C1, and the cells were collected at different time points (0, 24, 48, and 72 h) and subjected to flow cytometry analysis as mentioned in the methods. (C and D) Graphical representation of the FACS data presented in A and B, respectively. Percentage of apoptosis (A), S phase cells (S), G1 phase cells (G1), and G2 phase cells (G2) in C1-treated cells in A and B are calculated and shown in C and D, respectively.

less significantly (Figure 4D). These results indicate that the cytotoxicity of either of the compounds is increased by the presence of the other, suggesting that C1 and adriamycin work synergistically with each other.

In Vitro DNA Binding Behavior of C1. The binding of small molecules to DNA is conveniently monitored by changes in the fluorescence of substrates. The fluorescence of ethidium bromide (EtBr) increases significantly upon binding to double-stranded DNA, and its primary intercalation sites saturate when the ratio of DNA/EtBr reaches a value of 0.25.¹⁶ Addition of increasing amounts of C1 to a solution of DNA (calf thymus) containing EtBr (DNA/EtBr = 0.25) resulted in a concentration-dependent decrease of fluorescence, indicating the release of EtBr from the DNA (Figure 5A). When the C1/EtBr ratio is 1:1, the fluorescence intensity reduced by 10% from the saturation value. Further addition of another equivalent of C1 (C1/EtBr = 2) results in the decrease of fluorescence intensity by another 6%.

Next, we probed the interaction of adriamycin with DNA. We found that adriamycin fluorescence is quenched when it intercalates into DNA, confirming an earlier observation.¹⁷ In addition, we also probed the interaction of adriamycin with DNA in the presence of EtBr. Surprisingly, the binding of adriamycin to DNA appears

unaffected by the addition of EtBr (data not shown). This suggests that EtBr binding to DNA is independent of adriamycin binding to DNA.

Because the synergistic action between adriamycin and C1 is observed, it is of interest to probe if the binding of DNA with adriamycin is enhanced in the presence of C1. DNA was modified with two different concentrations of C1 for 24 h at room temperature, and addition of C1-modified DNA (C1-DNA) to adriamycin was monitored with fluorescence. Scatchard plots for the binding of adriamycin to DNA and C1-DNA based on fluorescence intensities are shown in Figure 5B. The Scatchard parameters were calculated following the procedure described before¹⁷ and are given in Table 3. The Scatchard plot for the binding of adriamycin to native DNA is linear, and the apparent binding constant (K) was found to be $0.49 \times 10^7 \text{ M}^{-1}$ (Figure 5B, Table 3). However, the Scatchard plots for the binding of adriamycin to C1-DNA are nonlinear (Figure 5B, Table 3). Further analysis as described before¹⁸ indicated that C1-DNA has two different binding sites for adriamycin. When the DNA/C1 ratio was 5.6, K_1 and K_2 were numerically evaluated to be 0.13×10^7 and $8.45 \times 10^7 \text{ M}^{-1}$, respectively. The apparent binding constant K_1 is in the similar range to that of adriamycin/native DNA. The second binding constant K_2 is associated with

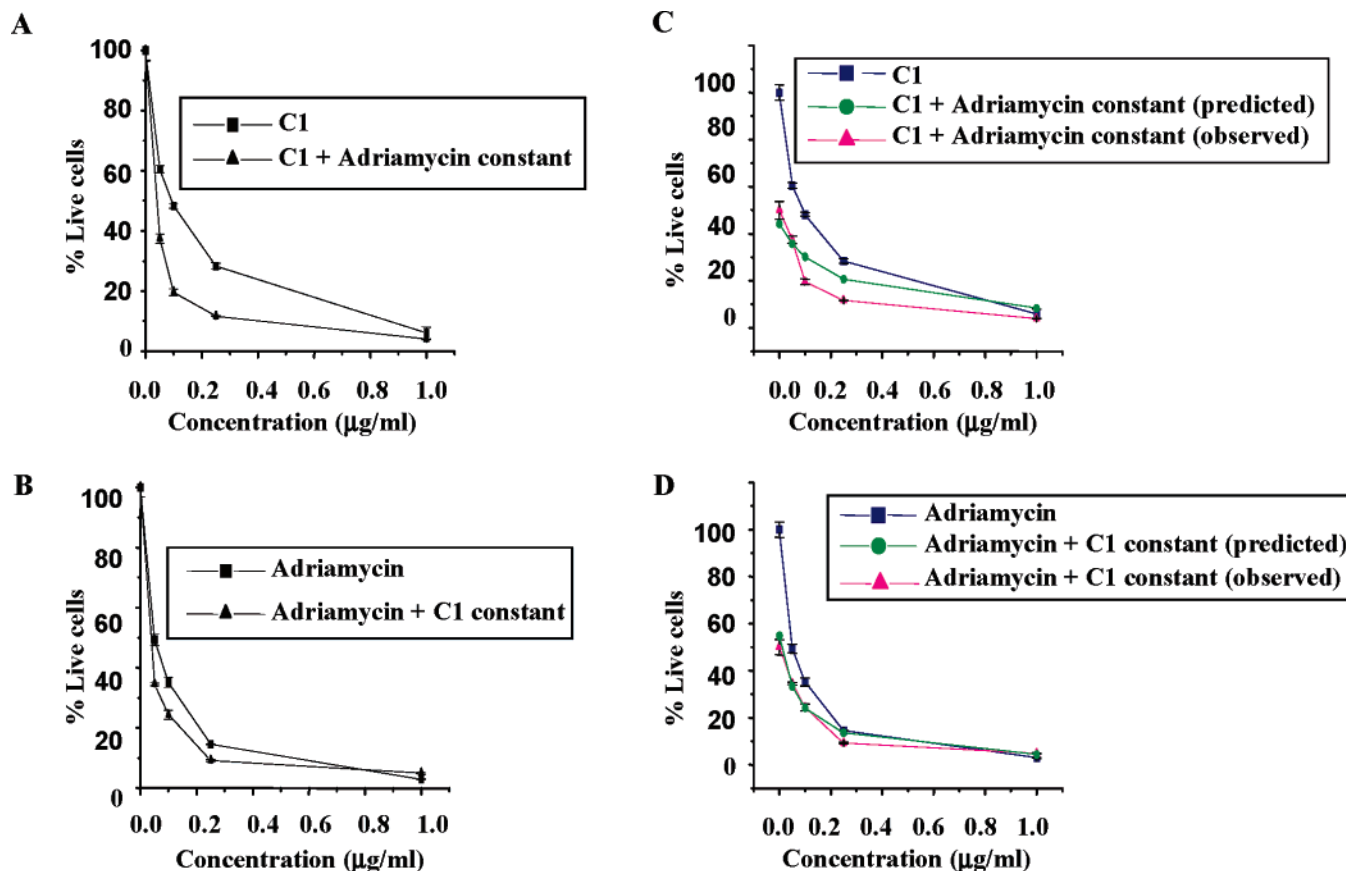


Figure 4. Synergism between C1 and adriamycin. (A and B) C1 and adriamycin synergistically increase the cytotoxicity of each other. (A) H460 cells were treated with increasing concentrations (0.05, 0.1, 0.25, and 1 $\mu\text{g}/\text{mL}$) of C1 and a constant amount (0.05 $\mu\text{g}/\text{mL}$) of adriamycin. (B) H460 cells were treated with increasing concentrations (0.05, 0.1, 0.25, and 1 $\mu\text{g}/\text{mL}$) of adriamycin and a constant amount (0.06 $\mu\text{g}/\text{mL}$) of C1. After 48 h of addition of these compounds, the proportion of live cells was quantified by the MTT assay as described in the Experimental Section. The absorbance of control cells was considered as 100%. (C and D) Experimental cytotoxicity curve and zero interaction response surface according to the dose additivity criterion for the combined action of adriamycin and C1 on H460 cells. Calculation of the response surface with the median function dose response relations. (C) The concentration of adriamycin is constant, and the concentration of C1 is varied. (D) The concentration of C1 is constant, and the concentration of adriamycin is varied.

adriamycin binding to regions of DNA modified by C1 and is significantly higher. This is further supported by the fact that K_2 increases to $16.7 \times 10^7 \text{ M}^{-1}$ when the DNA/C1 ratio is changed to 2.2. These results suggest that binding of adriamycin to DNA is significantly enhanced in the presence of C1.

Simulation Studies. Different models for the C1-DNA complex were constructed based on the binding preference of the metal complex C1 and the ability of nucleic acids to bind metal ions. The interaction of guanine residues through N7 has been shown to be ideal for binding metal ions. Removal of the ligand, acetonitrile, generates a vacant site on copper in C1. A model complex where N7 of guanine in a 17-mer strand of DNA binds to copper(I) of C1 is readily constructed using the program Hyperchem (Hypercube, Inc., Gainesville, FL). Because two copper ions are present, a two-pronged binding of DNA to C1 could also take place. The bifunctional binding mode of C1 was generated using the same 17-mer strand interacting through two guanine residues at G8 and G10 of the same strand, in the major groove. Similarly an interstrand complex was also constructed. The complex formed by the adducts of C1 were optimized following a procedure developed by Cox et al.¹⁹ using the program Hyperchem. Both monofunctional and bifunctional binding modes induce

significant changes in the conformation of DNA. The major changes are the disruption of the conventional hydrogen bonding between nearly five of the GC and AT base pairs adjacent to the binding site. Consequently, on binding to the metal complex, the base stacking and helical nature of DNA are disrupted, and the DNA strands are bent (Figure 6, parts B, C, and D). Base stacking distances increase from 4 Å to nearly 5.3 and 4.8 Å in intrastrand and interstrand cross-linked models, respectively. The stacking was completely disrupted in the monofunctional model. The helix angle between the two strands decreases from 180° in native DNA to 152°, 167°, and 157° in intrastrand, interstrand, and monofunctional models, respectively.

Discussion

We found in this study that C1 $[\text{Cu}_2(\text{DPPE})_3(\text{CH}_3\text{CN})_2(\text{ClO}_4)_2]$ is a potent inhibitor of cancer cell growth. C1 had an IC_{50} value in the range of adriamycin. We found C1 damaged DNA in vitro and activated the p53 pathway. We also show that inhibition of cancer cell growth involves both cell cycle arrest and apoptosis induction. In addition, C1 and adriamycin worked synergistically by potentiating the cytotoxicity of one by the other. Furthermore, we present evidence based on DNA binding and simulation studies for increased

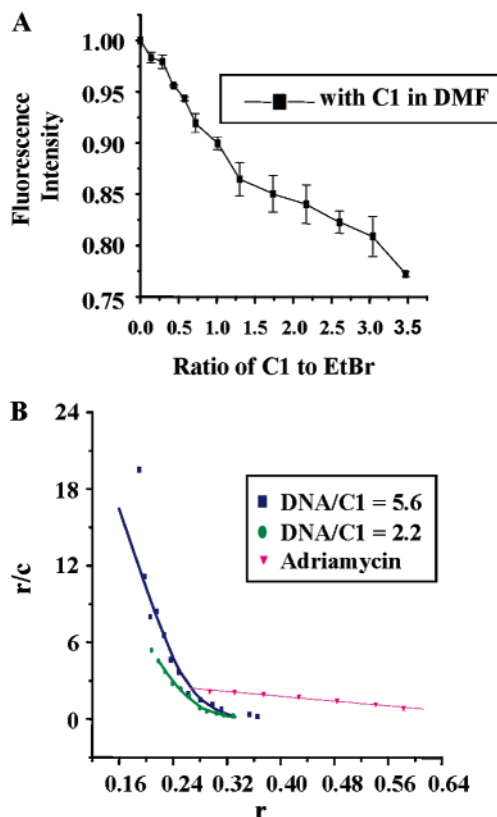


Figure 5. In vitro DNA binding behavior of C1. (A) Fluorescence quenching of DNA-bound EtBr by C1. Effect of addition of C1 to the emission intensity of the DNA-bound EtBr (5 and 15 μM respectively) at different ratios of the C1 to EtBr (0–3.5) in a 5 mM Tris-HCl/50 mM NaCl buffer (pH 7.2). The excitation wavelength was set to 510 nm. (B). Scatchard analysis of the binding of adriamycin with the native DNA and C1-bound DNA with different ratios of DNA/C1. The slope of the graph = $1/K$, and the value of r at $r/c = 0$ is the number of apparent binding sites. Addition of 17.5 μM DNA modified with 3.1 μM C1 and 13.5 μM DNA with 6.6 μM C1 to 2.6 μM adriamycin, when the ratio of DNA/C1 is 5.6 and 2, respectively, in a 5 mM Tris-HCl/50 mM NaCl buffer (pH 7.2). Excitation wavelength was set to 490 nm.

Table 3. Summary of the binding parameters of Adriamycin for CT DNA and C1-DNA^a

drug	DNA	K ($\times 10^7 \text{ M}^{-1}$)	n
adriamycin	CT-DNA	0.49 (0.23)	0.62

drug	DNA	K_1 ($\times 10^7 \text{ M}^{-1}$)	K_2 ($\times 10^7 \text{ M}^{-1}$)	n_1	n_2
adriamycin	DNA/C1 = 5.6	0.132	8.45	0.09	0.27
adriamycin	DNA/C1 = 2.2	0.37	16.7	0.09	0.25

^a K is the average binding constant, and n is the average number of binding sites.

binding of adriamycin to C1-DNA, thus providing a plausible mechanism for synergistic action between adriamycin and C1.

Metal complexes of DPPE have been shown to inhibit DNA polymerase α and cause DNA damage.^{4,20} Formation of COMETS in 90.3% of C1-treated cells in a single cell gel electrophoresis (COMET assay) suggests that C1 causes DNA damage in vitro. The tumor suppressor p53 gets activated in response to genotoxic stresses such as DNA damage, hypoxia, etc. leading to cell cycle arrest and induction of apoptosis.^{12,21} Our experiment suggests that C1 induces the levels of p53 in H460 cells. In

addition, C1-induced p53 is functional because p21, one of the p53 target genes, is also increased in C1-treated cells. Many chemotherapeutic drugs have been shown to perturb cell cycle progression^{22,23} and induce apoptosis.²⁴

[³H]Thymidine incorporation and flow cytometry experiments suggest that C1 treatment inhibits the cellular DNA synthesis and arrests the cells in the G1 and G2 phases of the cell cycle. Moreover, C1 treatment also resulted in induction of apoptosis. These results suggest that C1-mediated growth inhibition involves DNA damage, which in turn induces p53-mediated growth arrest and apoptosis.

The differences in the fluorescence intensities of bound and free EtBr are a sensitive probe for monitoring changes in the DNA structure. In the presence of C1, there is a decrease in the fluorescence intensity, showing release of EtBr from the DNA/EtBr complex. C1 distorts DNA in a fashion that reduces the efficiency with which DNA binds EtBr. However, it is found that the binding of adriamycin to DNA is unaffected by the presence of EtBr (data not shown). The observation regarding different regions of binding for EtBr and adriamycin is in agreement with a previous study²⁵ where fluorescence from terbium bound to DNA was quenched by adriamycin and not by EtBr. Clearly, the interactions of these two molecules with DNA are independent of one another. Taken in conjunction with the studies conducted with C1, these results point to the fact that C1 and adriamycin bind to different regions of DNA and could function independently and that the cytotoxic behavior of one drug may not affect the efficacy of the other adversely.

Direct evidence for the effect of C1 on the binding of adriamycin with DNA is obtained by studying the fluorescence of adriamycin in the presence of DNA modified by C1. The Scatchard plots suggest two different binding sites for Adriamycin in DNA-C1. Because the smaller binding constant is closer to the apparent binding constant calculated for native DNA ($K = 0.49 \times 10^7 \text{ M}^{-1}$), it is likely that it corresponds to the interaction of adriamycin with regions of DNA unaffected by C1. The larger K value belongs to the binding of adriamycin with DNA in regions modified by C1. Increasing the amount of C1 should increase the binding of adriamycin to DNA-C1. This conclusion is indeed supported by the experiments done with increased concentrations of C1 (DNA/C1 = 2.2). Thus, C1 clearly enhances the binding of adriamycin. So, on the basis of those two experiments, one can conclude that C1 and adriamycin bind to two different regions of DNA and that the modification of DNA with C1 can in fact increase the binding of adriamycin with DNA.

The simulation studies provide information on a possible mode of interaction between DNA and C1 and how the DNA structure is affected by binding to the metal complex. C1 is known to accommodate a variety of ligands in the coordination site generated by loss of acetonitrile. Formation of stable complexes by replacing acetonitrile in C1 with guanine residues suggests that the greater effectiveness of C1 is due to the presence of labile acetonitrile ligands. They are readily displaced by the nucleobases whereas there are no labile sites on the complexes C2 to C4. The possibility of binding C1

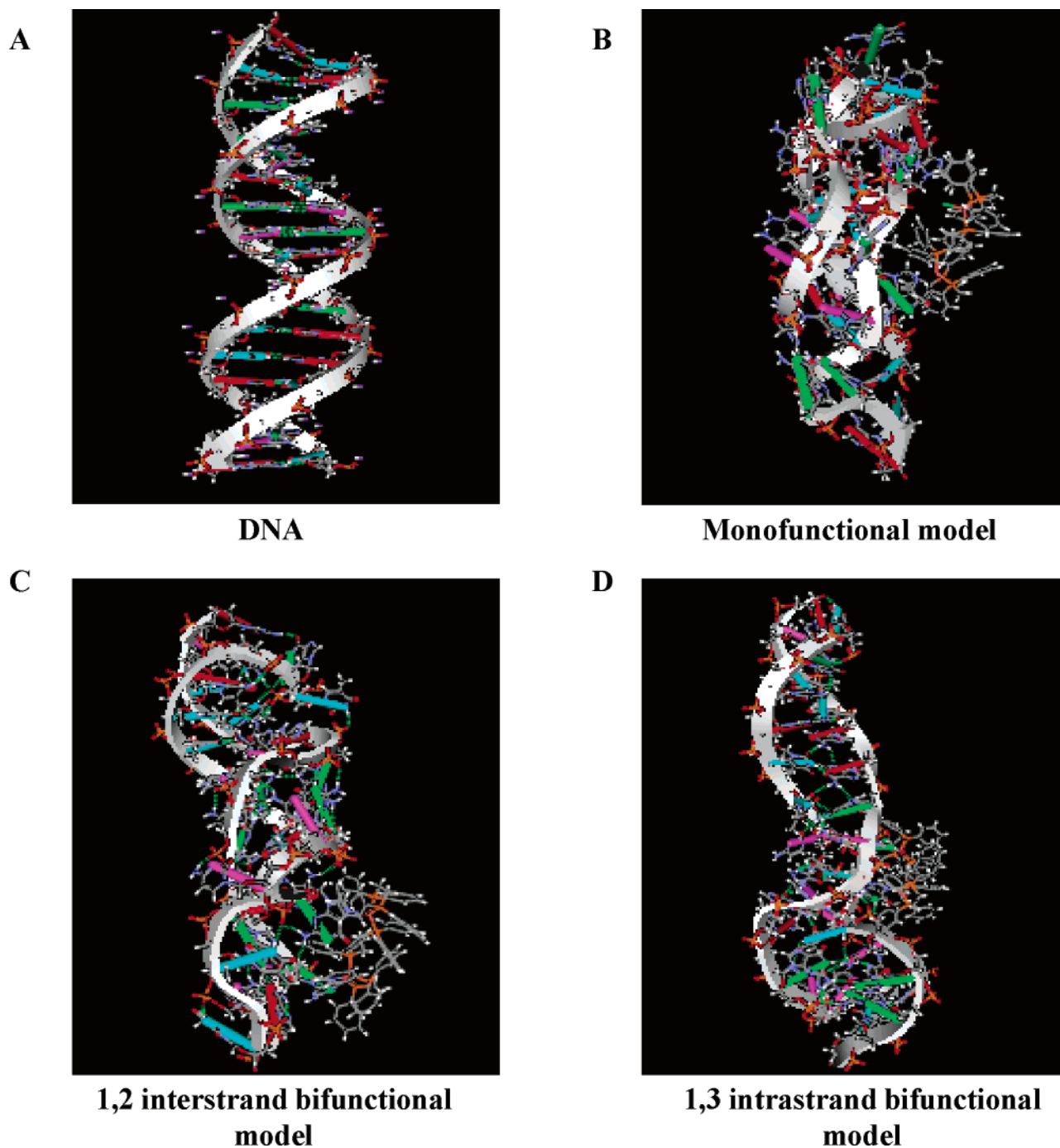


Figure 6. Simulated molecular model of duplex DNA (A). DNA bound in a monodentate fashion modified by a monofunctional adduct of C1 (B). Cross-linked by C1 1,3 intrastrand fashion (C). Monodentate binding of DNA to C1. Bidentate 1,2 intrastrand binding of DNA to C1. Bidentate 1,3 intrastrand cross-linking of DNA to C1. Copper of C1 is attached to N7 of guanine.

to two bases in the same strand explains why C1 binds better than other complexes and is more cytotoxic. Recent studies involving dinuclear copper(II) complexes²⁶ have also shown that dinuclear complexes are more active than mononuclear complexes. Modeling studies on the C1-bound DNA indicate significant distortions in the DNA strand. This is probably responsible for the enhancement in the binding of adriamycin with DNA.

A molecular level explanation for the effectiveness of C1, a dinuclear copper(I) phosphine complex, has been realized through a combination of flow cytometry, comet assays, thymidine incorporation, DNA binding, and simulation studies. Mechanistic studies have been

extremely valuable in arriving at a pathway by which C1 induces apoptosis. The cytotoxicity of C1 that has been found to function effectively against many different cell lines⁶ is due to its capability to interact with DNA. Fluorescence-based binding studies are valuable in arriving at the stability of substrate/DNA complexes. Simulation studies point out the possible ways by which DNA could bind to C1 very efficiently and, furthermore, the changes they bring about in the tertiary structure of DNA. Interestingly, the copper(I) complex can bind strongly to DNA and distort it if there are two guanine units suitably separated on the same strand. This two-pronged attack on DNA can significantly enhance the anticancer activity of the known drug adriamycin by

making DNA bind it better. Enhanced binding translates into enhanced activity as observed by the synergistic action of adriamycin and C1.

Multidrug chemotherapy that combines different types of chemotherapeutic agents can more effectively fight cancer. Our study shows that C1 and adriamycin increased the cytotoxicity of each other, suggesting that these compounds work synergistically. Thus, our study suggests that C1 could be considered for in vivo therapeutic testing either alone or in combination with adriamycin.

Experimental Section

General Methods. RPMI medium, penicillin, and streptomycin were obtained from GIBCO BRL (U.S.A.) Fetal calf serum and 3-(4,5-dimethylthiazol-2-yl)-2,5-diphenyltetrazolium bromide were products of Sigma Chemical Co. (U.S.A.). Sterile 96-well flat-bottom tissue-culture plates and other tissue-culture plastic wares were purchased from Tarsons (India). DPPE was obtained from Aldrich (U.S.A.). Dimethylsulfoxide (DMSO), dimethylformamide (DMF), and other chemicals were analytical grade reagents from Qualigens (India). Calf thymus DNA and ethidium bromide were bought from Sigma (U.S.A.). Human lung carcinoma cell line (H460) is maintained in RPMI 1640 medium containing 10% FCS.²⁷ The cultures were maintained in a 37 °C and 5% CO₂ incubator. Cu(CH₃CN)₄(ClO₄) (CAP) and C1 were synthesized using previously described methods.^{28,29} All reactions were carried out in an atmosphere of dry nitrogen using standard Schlenk and vacuum line techniques, and solvents were dried by standard methods. ¹H NMR spectra were recorded on a Bruker AMX 400 MHz spectrometer with tetramethylsilane as the internal reference. ³¹P{¹H} NMR spectra were recorded on a Bruker AMX 400 MHz spectrometer operating at 162 MHz. IR spectra were recorded in the solid state as KBr pellets on a Bruker Equinox 55 spectrometer. The stock solutions of complex C1 for mechanistic studies were prepared by dissolving the complex in 700 μL of DMF and 300 μL of tris-HCl buffer (pH 7.2).

Fluorescence Studies. Emission spectra were recorded with a Perkin-Elmer (LS 50B) fluorescence spectrometer using a 1 cm quartz cell at 22 °C. An excitation wavelength of 510 nm was used, and the emission of EtBr was monitored at 605 nm. The EtBr solution was taken in 5 mM tris-HCl buffer (pH 7.2) and 75 mM NaCl. The concentrations were 15 μM for EtBr and 5 μM for DNA in a total volume of 2.0 mL. This solution was subsequently titrated with various concentrations of C1 in DMF. Fluorescence emission intensities were corrected for dilution and quenching by the solvent, which was typically less than 5% of the observed intensities. For the adriamycin fluorescence quenching experiments, 17.5 μM DNA modified with 3.1 μM C1 and 13.5 μM DNA with 6.6 μM C1 was added to 2.6 μM adriamycin when the ratio of DNA/C1 is 5.6 and 2, respectively, in a 5 mM Tris-HCl/50 mM NaCl buffer (pH 7.2). Excitation wavelength for adriamycin was 490 nm, and emission was monitored at 590 nm.

Molecular Modeling. A double-stranded DNA model (17-mer) was constructed using the nucleic acids database of Hyperchem 7.0 to construct the B-form of DNA. The sequence of the complementary oligonucleotides is 5'-TGAATTC-GAGCTCGGTA-3' and 5'-TACCGAGCTCGAATTCA-3'. Counterions of charge +1.00 from Hyperchem's database were included at a distance of 0.167 nm from the phosphate oxygen of each base. The crystallographic coordinates of the closely related isostructural complex Cu₂(DPPE)₃Cl₂ were used to mimic C1 in the presence of chloride ions. Models of the monofunctional and bifunctional adduct were built by removing one or both chlorines to create a vacant site on copper. Copper was bonded to suitable ligands on the 17-mer. Two monofunctional adducts were formed in separate experiments from N7 of guanine (G5) and adenine (A12). A bifunctional adduct was generated using the N7 of guanine from G8 and

G10. To balance the charge, an appropriate number of sodium ions were deleted in the mono- and bifunctional adducts. The optimization was done in two steps by using the force field AMBER^{30,31} for the nucleic acid part and MM⁺³² all atom force field for the metal complex. A distance-dependent dielectric constant was used, which took care of the solvation parameter while van der Waals and electrostatic interactions were scaled by 0.5, Å which is a common practice in DNA modeling.³³ The resulting complexes were minimized with 1000 cycles of steepest descent, followed by up to 3000 steps of Polak–Ribiere conjugate-gradient minimization, until convergence was achieved as judged by the root mean square gradient being less than 0.03 kJ mol⁻¹ Å⁻¹. The optimized systems were then subjected to molecular dynamics simulations (1 fs time step, 30 ps at 300 K to achieve equilibrium). The cycle was repeated thrice before carrying out a final optimization using a 1000 step steepest descent and a conjugate gradient convergence.

Immunohistochemical Analysis. Immunohistochemical staining was performed as described before.²⁷ Cells were fixed after 24 h of addition of drugs and subjected to staining with mouse antihuman p53 monoclonal (Ab-2, Oncogene) and mouse antihuman p21^{WAF1/CIP1} monoclonal (Ab-1, Oncogene).

COMET Assay. The COMET assay was performed essentially as described previously.³⁴ Cells were harvested by trypsinization after treatment with adriamycin or C1 for 24 h and subjected to the COMET assay.

Cytotoxicity (MTT) Assay. The cytotoxicity exerted by compounds was checked by the MTT assay. The assay is based on the fact that only live cells reduce yellow 3-(4,5-dimethylthiazol-2-yl)-2,5-diphenyltetrazolium bromide (MTT) but not dead cells to blue formazan products. Cells were seeded in 96-well tissue-culture plates at 1200 cells/well in 100 μL of RPMI 1640 media. Cells were incubated overnight to adhere properly. Adriamycin and copper complexes were diluted to desired concentrations (0.05, 0.1, 0.25, and 1 μg/mL final concentration) in RPMI 1640 media and added to respective wells in triplicates and incubated for 2 days. At the end of 2 days, 20 μL of MTT (5 mg/mL in PBS) per well was added, and the plate was incubated for additional 3 h. The medium was decanted carefully, the formazan dye was dissolved in DMSO (200 μL/well), and absorption was read at 550 nm wavelength using a microplate reader ELISA spectrophotometer. The amount of the drug that kills 50% of cells (IC₅₀) was calculated for all of the compounds.

Cell Cycle Analysis. Cell cycle analysis was carried out as described before with minor modifications.³⁵ H460 cells were infected with varying concentrations of C1. At indicated time points, the cells were washed with PBS twice and harvested by trypsinization. The cells were washed again with PBS, fixed with cold 70% ethanol for 1 h, washed with PBS once, and then incubated with 4 μg of ribonuclease A (Roche) for 30 min at room temperature. Propidium iodide was added to the cell suspension at a final concentration of 20 μg/mL and incubated for 30 min. Cells were then analyzed by flow cytometry using FACScan (Becton Dickinson). The results were quantified by using the software Cell Quest (Becton Dickinson).

Acknowledgment. Generous financial support from DBT, New Delhi, India, is gratefully acknowledged. K.S. is a Wellcome Trust International senior research fellow.

Supporting Information Available: Preparation and spectroscopic characterization of complexes. This material is available free of charge via the Internet at <http://pubs.acs.org>.

References

- Sadler, P. J.; Guo, Z. Metal complexes in medicine: Design and mechanism of action. *Pure Appl. Chem.* **1998**, *70*, 863–871.
- Simon, T. M.; Kunishima, D. H.; Vibert, G. J.; Lober, A. Screening trial with the coordinated gold compound auranofin using mouse lymphocyte leukemia P388. *Cancer Res.* **1981**, *41*, 94–7.

- (3) Berners-Price, S. J.; Mirabelli, C. K.; Johnson, R. K.; Mattern, M. R.; McCabe, F. L.; Faucette, L. F.; Sung, C. M.; Mong, S. M.; Sadler, P. J.; Crooke, S. T. In vivo antitumor activity and in vitro cytotoxic properties of bis[1,2-bis(diphenylphosphino)ethane]gold(I) chloride. *Cancer Res.* **1986**, *46*, 5486–5489.
- (4) Snyder, R. M.; Mirabelli, C. K.; Johnson, R. K.; Sung, C. M.; Faucette, L. F.; McCabe, F. L.; Zimmerman, J. P.; Whitman, M.; Hempel, J. C.; Crooke, S. T. Modulation of the antitumor and biochemical properties of bis(diphenylphosphino)ethane with metals. *Cancer Res.* **1986**, *46*, 5054–5060.
- (5) Rankin, G. O. Nephrotoxicity induced by C- and N-arylsuccinimides. *J. Toxicol. Environ. Health B Crit. Rev.* **2004**, *7*, 399–416.
- (6) Adwankar, M. K.; Wycliff, C.; Samuelson, A. G. In vitro cytotoxic effect of new diphenylphosphinoethane–copper(I) complexes on human ovarian carcinoma cell lines. *Indian J. Exp. Biol.* **1997**, *35*, 810–814.
- (7) Van der Veer, J. L.; Reedijk, J. Investigating antitumor drug mechanisms. *Chem. Br.* **1988**, 775–780.
- (8) Pillarsetty, N.; Katti, K. K.; Hoffman, T. J.; Volkert, W. A.; Katti, K. V.; Kamei, H.; Koide, T. In vitro and in vivo antitumor properties of tetrakis(trihydroxy-methyl)phosphinesgold(I) chloride. *J. Med. Chem.* **2003**, *46*, 1130–1132.
- (9) Chlopkiewicz, B. Evaluation of adriamycin induced DNA damage and repair in human and animal cells. *Acta Pol. Pharm.* **2002**, *59*, 115–20.
- (10) Anuszevska, E. L.; Gruber, B. DNA damage and repair in normal and neoplastic cells treated with adriamycin. *Acta Biochim. Pol.* **1995**, *41*, 385–90.
- (11) Tewey, K. M.; Rowe, T. C.; Yang, L.; Halligan, B. D.; Liu, L. F. Adriamycin-induced DNA damage mediated by mammalian DNA topoisomerase II. *Science* **1984**, *226*, 466–8.
- (12) Levine, A. J. p53, the cellular gatekeeper for growth and division. *Cell* **1997**, *88*, 323–331.
- (13) Einhorn, L. H. Curing metastatic testicular cancer. *Proc. Natl. Acad. Sci. U.S.A.* **2002**, *99*, 7, 4592–4595.
- (14) Suhnel, J. Parallel dose–response curves in combination experiments. *Bull. Math. Biol.* **1998**, *60*, 197–213.
- (15) Berman, E.; Chang, T. T. Selective synergism against the target versus host bone marrow progenitor cells. In *Synergism and Antagonism in Chemotherapy*; Chou, T.-C., Rideout, D. C., Eds.; Academic Press: San Diego, 1991; pp 715–737.
- (16) Brabec, V.; Kasparkova, J.; Vrana, O.; Novakova, O.; Cox, J. W.; Ou, Y.; Farrell, N. DNA modifications by a novel bifunctional trinuclear platinum phase I anticancer agent. *Biochemistry* **1999**, *38*, 6781–6790.
- (17) Virgil, H.; Du Vernay, Jr.; Pachter, J. A.; Crooke, S. T. Deoxyribonucleic acid binding studies on several new anthracycline antibiotics. Sequence preference and structure–activity relationships of marcellomycin and its analogues as compared to adriamycin. *Biochemistry* **1979**, *18*, 4024–4030.
- (18) Klotz, I. M.; Hunston, D. L. Properties of graphical representations of multiple classes of binding sites. *Biochemistry* **1971**, *10*, 3065–3069.
- (19) Cox, J. W.; Berners-Price, S. J.; Derray, M.; Davies, S.; Yun, Q.; Farrell, N. Kinetic analysis of the stepwise formation of a long-range DNA interstrand cross-link by a dinuclear platinum antitumor complex: Evidence for aquated intermediates and formation of both kinetically and thermodynamically controlled conformers. *J. Am. Chem. Soc.* **2001**, *123*, 1316–1326.
- (20) Mirabelli, C. K.; Johnson, R. K.; Hill, D. T.; Faucette, L.; Girard, G.; Kuo, G.; Sung, C.-M.; Crooke, S. T. Correlation of in vitro cytotoxic and in vivo antitumor activities of gold(I) coordination complexes. *J. Med. Chem.* **1986**, *29*, 218–223.
- (21) Somasundaram, K.; El-Deiry, W. S. Tumor suppressor p53: Regulation and function. *Front. Biosci.* **2000**, *5*, d424–437.
- (22) Webster, K. R. Therapeutic potential of targeting the cell cycle. *Chem. Res. Toxicol.* **2000**, *13*, 940–943.
- (23) Sherri C. J. The Pezcoller lecture: Cancer cell cycles revisited. *Cancer Res.* **2000**, *60*, 3689–3695.
- (24) Johnstone, R. W.; Ruefli, A. A.; Lowe, S. W. Apoptosis: A link between cancer genetics and chemotherapy. *Cell* **2002**, *108*, 153–164.
- (25) Zunino, F.; Gambetta, R.; Di Marco, A.; Zaccara, A. Interaction of daunomycin and its derivatives with DNA. *Biochim. Biophys. Acta* **1981**, *656*, 167–176.
- (26) Gonzalez-Alvarez, M.; Alzuet, G.; Borrás, J.; Pitie, M.; Meunier, B. DNA Cleavage Studies of Mononuclear and Dinuclear copper(I) complexes with benzothiazolesulfonamide ligands. *JBIC, J. Biol. Inorg. Chem.* **2003**, *8*, 644–652.
- (27) Das, S.; El-Deiry, W. S.; Somasundaram, K. Efficient growth inhibition of HPV E6-expressing cells by an adenovirus expressing p53 homologue p73b. *Oncogene* **2003**, *22*, 8394–8402.
- (28) Hathaway, B. J.; Holah, D. G.; Postlethwaite, J. D. The preparation and properties of some tetrakis(methyl cyanide)copper(I) complexes. *J. Chem. Soc., Dalton Trans.* **1961**, 3215–18.
- (29) Vijayashree, N.; Samuelson, A. G.; Nethaji, M. 1,2-Bis(diphenylphosphino)ethane(dppe) bridged dinuclear copper(I) complexes: Investigations of solid state and solution structures by CP/MAS 31P NMR spectroscopy, X-ray crystallography, IR spectroscopy and solution 31P and 65Cu NMR spectroscopy. *Curr. Sci.* **1993**, *65*, 57–67.
- (30) Weiner, S. J.; Kollman, P. A.; Singh, U. C.; Ghio, C.; Alagona, G.; Profeta, S., Jr.; Weiner, P. A new force field for molecular mechanical simulation of nucleic acids and proteins. *J. Am. Chem. Soc.* **1984**, *106*, 765–784.
- (31) Weiner, S. J.; Kollman, P. A.; Nguyen, D. T.; Case, D. A. An all atom force field for simulations of proteins and nucleic acids. *J. Comput. Chem.* **1986**, *7*, 230–52.
- (32) Allinger, N. L. Conformational analysis. 130. MM2. a hydrocarbon force field utilizing V1 and V2 torsional terms. *J. Am. Chem. Soc.* **1977**, *99*, 8127–34.
- (33) Orozco, M.; Laughton, C. A.; Herzyk, P.; Neidle, S. Molecular mechanics modeling of drug–DNA structures; the effects of differing dielectric treatment on helix parameters and comparison with a solvated structural model. *J. Biomol. Struct. Dyn.* **1990**, *8*, 359–371.
- (34) Tice, R. R.; Agurell, E.; Anderson, D.; Burlinson, B.; Hartmann, A.; Kobayashi, H.; Miyamae, Y.; Rojas, E.; Ryu, J. C.; Sasaki, Y. F. Single Cell Gel/Comet Assay: Guidelines for In Vitro and In Vivo Genetic Toxicology Testing. *Environ. Mol. Mutagen.* **2000**, *35*, 206–221.
- (35) Wajapeyee, N.; Somasundaram, K. Cell cycle arrest and apoptosis induction by Activator protein 2 α (AP-2 α) and the role of p53 and p21WAF1/CIP1 in AP-2 α . Mediated growth inhibition. *J. Biol. Chem.* **2003**, *278*, 52093–52101.

JM049430G